

Introduction and Overview

1

1.1 Scope of the Subject and Recent Highlights

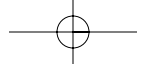
Atmospheric science is a relatively new, applied discipline that is concerned with the structure and evolution of the planetary atmospheres and with the wide range of phenomena that occur within them. To the extent that it focuses mainly on the Earth's atmosphere, atmospheric science can be regarded as one of the *Earth or geosciences*, each of which represents a particular fusion of elements of physics, chemistry, and fluid dynamics.

The historical development of atmospheric sciences, particularly during the 20th century, has been driven by the need for more accurate weather forecasts. In popular usage the term “meteorologist,” a synonym for atmospheric scientist, means “weather forecaster.” During the past century, weather forecasting has evolved from an art that relied solely on experience and intuition into a science that relies on numerical models based on the conservation of mass, momentum, and energy. The increasing sophistication of the models has led to dramatic improvements in forecast skill, as documented in Fig. 1.1. Today’s weather forecasts address not only the deterministic, day-to-day evolution of weather patterns over the course of the next week or two, but also the likelihood of hazardous weather events (e.g., severe thunderstorms, freezing rain) on an hour-by-hour basis (so called

“nowcasting”), and departures of the climate (i.e., the statistics of weather) from seasonally adjusted normal values out to a year in advance.

Weather forecasting has provided not only the intellectual motivation for the development of atmospheric science, but also much of the infrastructure. What began in the late 19th century as an assemblage of regional collection centers for real time teletype transmissions of observations of surface weather variables has evolved into a sophisticated *observing system* in which satellite and in situ measurements of many surface and upper air variables are merged (or *assimilated*) in a dynamically consistent way to produce optimal estimates of their respective three-dimensional fields over the entire globe. This global, real time atmospheric dataset is the envy of oceanographers and other geo- and planetary scientists: it represents both an extraordinary technological achievement and an exemplar of the benefits that can derive from international cooperation. Today’s global weather observing system is a vital component of a broader Earth observing system, which supports a wide variety of scientific endeavors, including climate monitoring and studies of ecosystems on a global scale.

A newer, but increasingly important organizing theme in atmospheric science is *atmospheric chemistry*. A generation ago, the principal focus of this field was urban air quality. The field experienced



2 Introduction and Overview

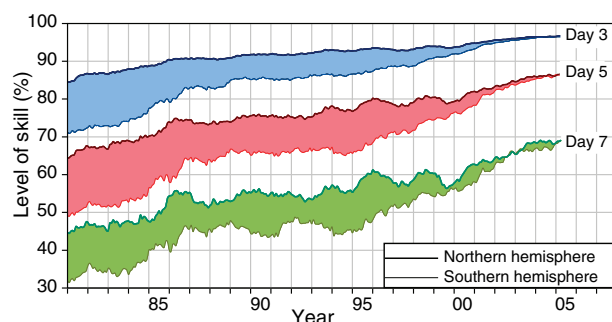


Fig. 1.1 Improvement of forecast skill with time from 1981 to 2003. The ordinate is a measure of forecast skill, where 100% represents a perfect forecast of the hemispheric flow pattern at the 5-km level. The upper pair of curves is for 3-day forecasts, the middle pair for 5-day forecasts, and the lower pair for 7-day forecasts. In each pair, the upper curve that marks the top of the band of shading represents the skill averaged over the northern hemisphere and the lower curve represents the skill averaged over the southern hemisphere. Note the continually improving skill levels (e.g., today's 5-day forecasts of the northern hemisphere flow pattern are nearly as skillful as the 3-day forecasts of 20 years ago). The more rapid increase in skill in the southern hemisphere reflects the progress that has been made in assimilating satellite data into the forecast models. [Updated from *Quart. J. Royal Met. Soc.*, **128**, p. 652 (2002). Courtesy of the European Centre for Medium-Range Weather Forecasting.]

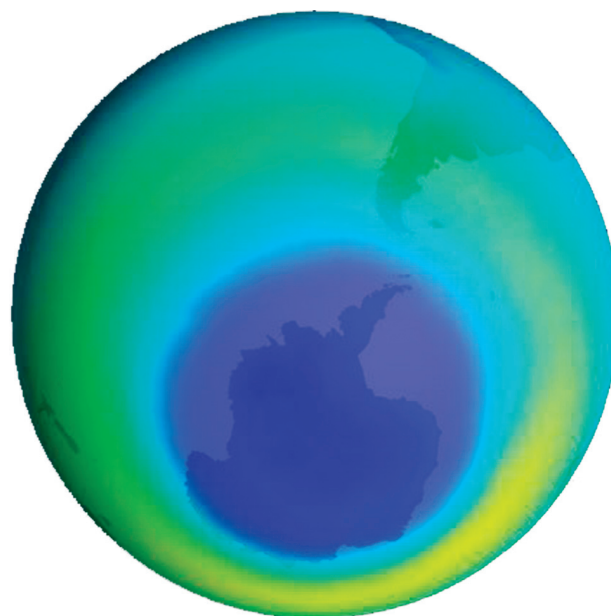


Fig. 1.2 The Antarctic ozone hole induced by the buildup of synthetic chlorofluorocarbons, as reflected in the distribution of vertically integrated ozone over high latitudes of the southern hemisphere in September, 2000. Blue shading represents substantially reduced values of total ozone relative to the surrounding region rendered in green and yellow. [Based on data from NASA TOMS Science Team; figure produced by NASA's Scientific Visualization Studio.]

a renaissance during the 1970s when it was discovered that forests and organisms living in lakes over parts of northern Europe, the northeastern United States, and eastern Canada were being harmed by *acid rain* caused by sulfur dioxide emissions from coal-fired electric power plants located hundreds and, in some cases, thousands of kilometers upwind. The sources of the acidity are gaseous oxides of sulfur and nitrogen (SO_2 , NO , NO_2 , and N_2O_5) that dissolve in microscopic cloud droplets to form weak solutions of sulfuric and nitric acids that may reach the ground as raindrops.

There is also mounting evidence of the influence of human activity on the composition of the global atmosphere. A major discovery of the 1980s was the *Antarctic “ozone hole”*: the disappearance of much of the stratospheric ozone layer over the southern polar cap each spring (Fig. 1.2). The ozone destruction was found to be caused by the breakdown of chlorofluorocarbons (CFCs), a family of synthetic gases that was becoming increasingly

widely used for refrigeration and various industrial purposes. As in the acid rain problem, heterogeneous chemical reactions involving cloud droplets were implicated, but in the case of the “ozone hole” they were taking place in wispy polar stratospheric clouds. Knowledge gained from atmospheric chemistry research has been instrumental in the design of policies to control and ultimately reverse the spread of acid rain and the ozone hole. The unresolved scientific issues surrounding *greenhouse warming* caused by the buildup of carbon dioxide (Fig. 1.3) and other trace gases released into the atmosphere by human activities pose a new challenge for atmospheric chemistry and for the broader field of geochemistry.

Atmospheric science also encompasses the emerging field of *climate dynamics*. As recently as a generation ago, climatic change was viewed by most atmospheric scientists as occurring on such long timescales that, for most purposes, today's climate could be described in terms of a standard set of

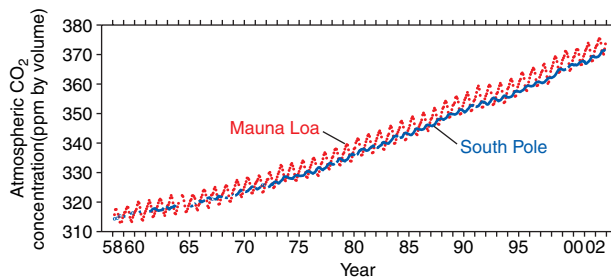


Fig. 1.3 Time series showing the upward trend in monthly mean atmospheric CO₂ concentrations (in parts per million by volume) at Mauna Loa and the South Pole due to the burning of fossil fuels. A pronounced annual cycle is also evident at Mauna Loa, with minimum values in the summer. [Based on data of C. D. Keeling. Courtesy of Todd P. Mitchell.]

statistics, such as January climatological-mean (or “normal”) temperature. In effect, climatology and climate change were considered to be separate subfields, the former a branch of atmospheric sciences and the latter largely the province of disciplines such as geology, paleobotany, and geochemistry. Among the factors that have contributed to the emergence of a more holistic, dynamic view of climate are:

- documentation of a coherent pattern of year-to-year climate variations over large areas of the globe that occurs in association with El Niño (Section 10.2).
- proxy evidence, based on a variety of sources (ocean sediment cores and ice cores, in particular), indicating that large, spatially coherent climatic changes have occurred on time scales of a century or even less (Section 2.6.4).
- the rise of the global-mean surface air temperature during the 20th century and projections of a larger rise during the 21st century due to human activities (Section 10.4).

Like some aspects of atmospheric chemistry, climate dynamics is inherently multidisciplinary: to understand

the nature and causes of climate variability, the atmosphere must be treated as a component of the *Earth system*.

1.2 Some Definitions and Terms of Reference

Even though the Earth is not perfectly spherical, atmospheric phenomena are adequately represented in terms of a spherical coordinate system, rotating with the Earth, as illustrated in Fig. 1.4. The coordinates are latitude ϕ , longitude λ , and height z above sea level, z .¹ The angles are often replaced by the distances

$$dx \equiv r d\lambda \cos \phi \quad (1.1)$$

and

$$dy \equiv r d\phi$$

where x is distance east of the Greenwich meridian along a latitude circle, y is distance north of the

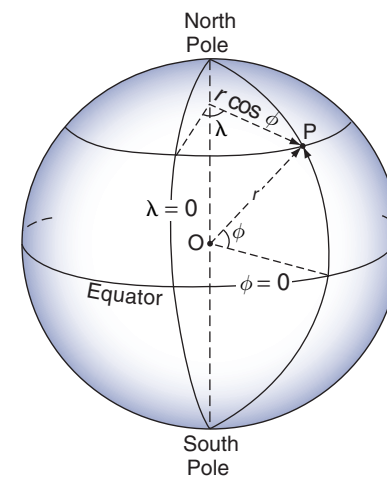
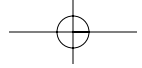


Fig. 1.4 Coordinate system used in atmospheric science. Angle ϕ is latitude, defined as positive in the northern hemisphere and negative in the southern hemisphere, and λ is longitude relative to the Greenwich meridian, positive eastward. The radial coordinate (not shown) is height above sea level.

¹ Oceanographers and applied mathematicians often use the colatitude $\theta = \pi/2 - \phi$ instead of ϕ .



4 Introduction and Overview



Fig. 1.5 The limb of the Earth, as viewed from space in visible satellite imagery. The white layer is mainly light scattered from atmospheric aerosols and the overlying blue layer is mainly light scattered by air molecules. [NASA Gemini-4 photo. Photograph courtesy of NASA.]

equator, and r is the distance from the center of the Earth. At the Earth's surface a degree of latitude is equivalent to 111 km (or 60 nautical miles). Because 99.9% of the mass of the atmosphere is concentrated within the lowest 50 km, a layer with a thickness less than 1% of the radius of the Earth, r , is nearly always replaced by the mean radius of the Earth (6.37×10^6 m), which we denote by the symbol R_E . Images of the limb of the Earth (Fig. 1.5) emphasize how thin the atmosphere really is.

The three velocity components used in describing atmospheric motions are defined as

$$u \equiv \frac{dx}{dt} = R_E \cos \phi \frac{d\lambda}{dt} \quad (\text{the zonal velocity component}) \quad (1.2)$$

$$v \equiv \frac{dy}{dt} = R_E \frac{d\phi}{dt} \quad (\text{the meridional velocity component}),$$

and

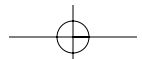
$$w \equiv \frac{dz}{dt} = \frac{dr}{dt} \quad (\text{the vertical velocity component}).$$

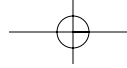
where z is height above mean sea level. The adjectives *zonal* and *meridional* are also commonly used in reference to averages, gradients, and cross sections. For example, a *zonal average* denotes an average around latitude circles; a *meridional cross section* denotes a north–south slice through the atmosphere. The *horizontal velocity vector* \mathbf{V} is given by $\mathbf{V} \equiv u\mathbf{i} + v\mathbf{j}$, where \mathbf{i} and \mathbf{j} are the unit vectors in the zonal and meridional directions, respectively. Positive and negative zonal velocities are referred to as *westerly* (from the west) and *easterly* (from the east) winds, respectively; positive and negative meridional velocities are referred to as *southerly* and *notherly* winds (in both northern and southern hemispheres, respectively).² For scales of motion in the Earth's atmosphere in excess of 100 km, the length scale greatly exceeds the depth scale, and typical magnitudes of the horizontal velocity component \mathbf{V} exceed those of the vertical velocity component w by several orders of magnitude. For these scales the term *wind* is synonymous with *horizontal velocity component*. The SI unit for velocity (or speed) is m s^{-1} . One meter per second is equivalent to 1.95 knots (1 knot = 1 nautical mile per hour). Vertical velocities in large-scale atmospheric motions are often expressed in units of cm s^{-1} : 1 cm s^{-1} is roughly equivalent to a vertical displacement of 1 kilometer per day.

Throughout this book, the local derivative $\partial/\partial t$ refers to the rate of change at a fixed point in rotating (x, y, z) space and the total time derivative d/dt refers to the rate of change following an air parcel as it moves along its three-dimensional trajectory through the atmosphere. These so-called *Eulerian*³

² Dictionaries offer contradictory definitions of these terms, derived from different traditions.

³ **Leonhard Euler** (1707–1783) Swiss mathematician. Held appointments at the St. Petersburg Academy of Sciences and the Berlin Academy. Introduced the mathematical symbols e , i , and $f(x)$. Made fundamental contributions in optics, mechanics, electricity, and magnetism, differential equations, and number theory. First to describe motions in a rotating coordinate system. Continued to work productively after losing his sight by virtue of his extraordinary memory.





1.2 Some Definitions and Terms of Reference 5

and *Lagrangian*⁴ rates of change are related by the chain rule

$$\frac{d}{dt} = \frac{\partial}{\partial t} + u \frac{\partial}{\partial x} + v \frac{\partial}{\partial y} + w \frac{\partial}{\partial z}$$

which can be rewritten in the form

$$\frac{\partial}{\partial t} = \frac{d}{dt} - u \frac{\partial}{\partial x} - v \frac{\partial}{\partial y} - w \frac{\partial}{\partial z} \quad (1.3)$$

The terms involving velocities in Eq. (1.3), including the minus signs in front of them, are referred to as *advection terms*. At a fixed point in space the Eulerian and Lagrangian rates of change of a variable ψ differ by virtue of the advection of air from upstream, which carries with it higher or lower values of ψ . For a hypothetical *conservative tracer*, the Lagrangian rate of change is identically equal to zero, and the Eulerian rate of change is

$$\frac{\partial}{\partial t} = -u \frac{\partial}{\partial x} - v \frac{\partial}{\partial y} - w \frac{\partial}{\partial z}$$

The fundamental thermodynamic variables are pressure p , density ρ , and temperature T . The SI unit

of pressure is $1 \text{ N m}^{-2} = 1 \text{ kg m}^{-1} \text{ s}^{-2} = 1 \text{ pascal (Pa)}$. Prior to the adoption of SI units, atmospheric pressure was expressed in millibars (mb), where $1 \text{ bar} = 10^6 \text{ g cm}^{-1} \text{ s}^{-2} = 10^6 \text{ dynes}$. In the interests of retaining the numerical values of pressure that atmospheric scientists and the public have become accustomed to, atmospheric pressure is usually expressed in units of hundreds of (i.e., hecto) pascals (hPa).⁵ Density is expressed in units of kg m^{-3} and temperature in units of $^{\circ}\text{C}$ or K, depending on the context, with $^{\circ}\text{C}$ for temperature differences and K for the values of temperature itself. Energy is expressed in units of joules ($\text{J} = \text{kg m}^2 \text{ s}^{-2}$).

Atmospheric phenomena with timescales shorter than a few weeks, which corresponds to the theoretical limit of the range of deterministic (day-by-day) weather forecasting, are usually regarded as relating to *weather*, and phenomena on longer timescales as relating to *climate*. Hence, the adage (intended to apply to events a month or more in the future): “Climate is what you expect; weather is what you get.” Atmospheric variability on timescales of months or longer is referred to as *climate variability*, and statistics relating to conditions in a typical (as opposed to a particular) season or year are referred to as *climatological-mean* statistics.

1.1 Atmospheric Predictability and Chaos

Atmospheric motions are inherently unpredictable as an initial value problem (i.e., as a system of equations integrated forward in time from specified initial conditions) beyond a few weeks. Beyond that time frame, uncertainties in the forecasts, no matter how small they might be in the initial conditions, become as large as the observed variations in atmospheric flow patterns. Such exquisite *sensitivity to initial conditions* is characteristic of a broad class of mathematical models of real phenomena, referred to as *chaotic nonlinear systems*. In fact, it was the growth of errors in a highly simplified

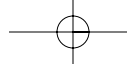
weather forecast model that provided one of the most lucid early demonstrations of this type of behavior.

In 1960, Professor Edward N. Lorenz in the Department of Meteorology at MIT decided to rerun an experiment with a simplified atmospheric model in order to extend his “weather forecast” farther out into the future. To his surprise, he found that he was unable to duplicate his previous forecast. Even though the code and the prescribed initial conditions in the two experiments were identical, the states of the model in the two fore-

Continued on next page

⁴ Joseph Lagrange (1736–1813) French mathematician and mathematical physicist. Served as director of the Berlin Academy, succeeding Euler in that role. Developed the calculus of variations and also made important contributions to differential equations and number theory. Reputed to have told his students “Read Euler, read Euler, he is our master in everything.”

⁵ Although the pressure will usually be expressed in hectopascals (hPa) in the text, it should be converted to pascals (Pa) when working quantitative exercises that involve a mix of units.



6 Introduction and Overview

1.1 Continued

casts diverged, over the course of the first few hundred time steps, to the point that they were no more like one another than randomly chosen states in experiments started from entirely different initial conditions. Lorenz eventually discovered that the computer he was using was introducing round-off errors in the last significant digit that were different each time he ran the experiment. Differences between the “weather patterns” in the different runs were virtually indistinguishable at first, but they grew with each time step until they eventually became as large as the range of variations in the individual model runs.

Lorenz’s model exhibited another distinctive and quite unexpected form of behavior. For long periods of (simulated) time it would oscillate around some “climatological-mean” state. Then, for no apparent reason, the state of the model would undergo an abrupt “regime shift” and begin to oscillate around another quite different state, as illustrated in Fig. 1.6. Lorenz’s model exhibited two such preferred “climate regimes.” When the state of the model resided within one of these regimes, the “weather” exhibited quasi-periodic oscillations and consequently was predictable quite far into the future. However, the shifts between regimes were abrupt, irregular, and inherently unpredictable beyond a few simulated days. Lorenz referred to the two climates in the model as *attractors*.

The behavior of the real atmosphere is much more complicated than that of the highly simplified model used by Lorenz in his experiments. Whether the Earth’s climate exhibits such regime-like behavior, with multiple “attractors,” or whether it should be viewed as varying about a single state that varies in time in response to solar, orbital, volcanic, and anthropogenic forcing is a matter of ongoing debate.

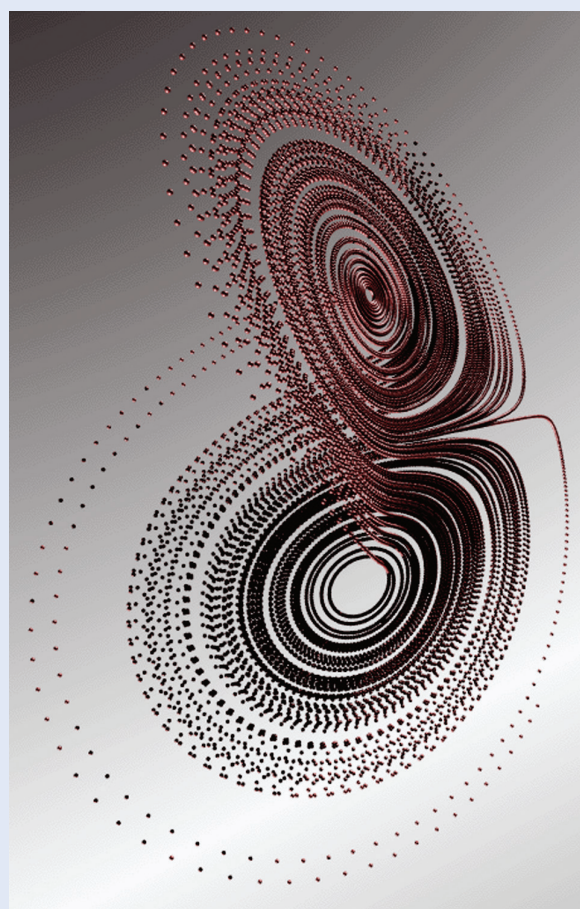


Fig. 1.6 The history of the state of the model used by Lorenz can be represented as a trajectory in a three-dimensional space defined by the amplitudes of the model’s three dependent variables. Regime-like behavior is clearly apparent in this rendition. Oscillations around the two different “climate attractors” correspond to the two, distinctly different sets of spirals, which lie in two different planes in the three-dimensional phase space. Transitions between the two regimes occur relatively infrequently. [Permission to use figure from *Nature*, 406, p. 949 (2000). © Copyright 2000 Nature Publishing Group. Courtesy of Paul Bourke.]

1.3 A Brief Survey of the Atmosphere

The remainder of this chapter provides an overview of the optical properties, composition, and vertical structure of the Earth’s atmosphere, the major wind systems, and the climatological-mean distribution of precipitation. It introduces some of the terminology that will be used in subsequent chapters and some of

the conventions that will be used in performing calculations involving amounts of mass and rates of movement.

1.3.1 Optical Properties

The Earth’s atmosphere is relatively transparent to incoming solar radiation and opaque to outgoing radiation emitted by the Earth’s surface. The blocking

of outgoing radiation by the atmosphere, popularly referred to as the *greenhouse effect*, keeps the surface of the Earth warmer than it would be in the absence of an atmosphere. Much of the absorption and re-emission of outgoing radiation are due to air molecules, but cloud droplets also play a significant role. The radiation emitted to space by air molecules and cloud droplets provides a basis for remote sensing of the three-dimensional distribution of temperature and various atmospheric constituents using satellite-borne sensors.

The atmosphere also scatters the radiation that passes through it, giving rise to a wide range of optical effects. The blueness of the outer atmosphere in Fig. 1.5 is due to the preferential scattering of incoming short wavelength (solar) radiation by air molecules, and the whiteness of lower layers is due to scattering from cloud droplets and atmospheric aerosols (i.e., particles). The backscattering of solar radiation off the top of the deck of low clouds off the California coast in Fig. 1.7 greatly enhances the

whiteness (or reflectivity) of that region as viewed from space. Due to the presence of clouds and aerosols in the Earth's atmosphere, $\sim 22\%$ of the incoming solar radiation is backscattered to space without being absorbed. The backscattering of radiation by clouds and aerosols has a cooling effect on climate at the Earth's surface, which opposes the greenhouse effect.

1.3.2 Mass

At any point on the Earth's surface, the atmosphere exerts a downward force on the underlying surface due to the Earth's gravitational attraction. The downward force, (i.e., the *weight*) of a unit volume of air with density ρ is given by

$$F = \rho g \quad (1.4)$$

where g is the acceleration due to gravity. Integrating Eq. (1.4) from the Earth's surface to the "top" of the atmosphere, we obtain the atmospheric pressure on the Earth's surface p_s due to the weight (per unit area) of the air in the overlying column

$$p_s = \int_0^{\infty} \rho g dz \quad (1.5)$$

Neglecting the small variation of g with latitude, longitude and height, setting it equal to its mean value of $g_0 = 9.807 \text{ m s}^{-2}$, we can take it outside the integral, in which case, Eq. (1.5) can be written as

$$p_s = mg_0 \quad (1.6)$$

where $m = \int_0^{\infty} \rho dz$ is the vertically integrated mass per unit area of the overlying air.

Exercise 1.1 The globally averaged surface pressure is 985 hPa. Estimate the mass of the atmosphere.

Solution: From Eq. (1.6), it follows that

$$\bar{m} = \frac{\bar{p}_s}{g_0}$$

where the overbars denote averages over the surface of the Earth. In applying this relationship the pressure

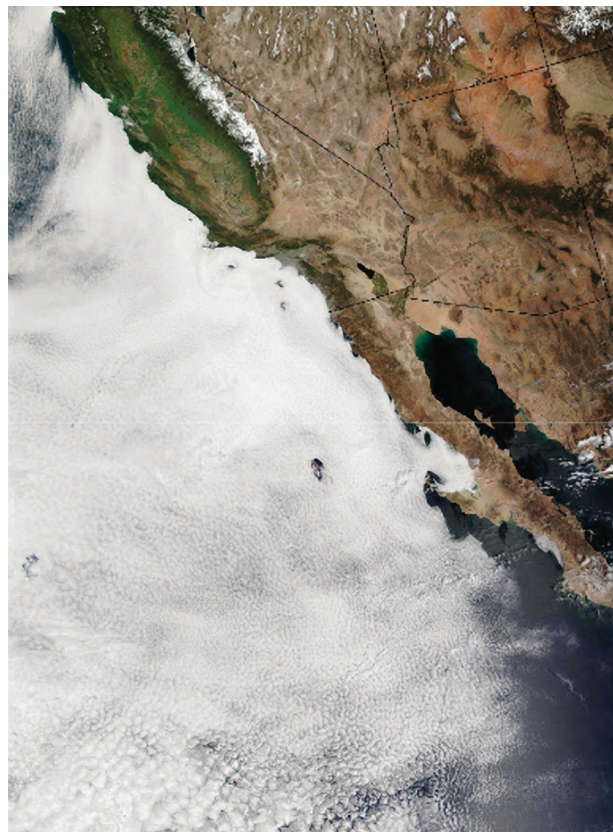
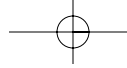


Fig. 1.7 A deck of low clouds off the coast of California, as viewed in reflected visible radiation. [NASA MODIS imagery. Photograph courtesy of NASA.]



8 Introduction and Overview

must be expressed in pascals (Pa). Substituting numerical values we obtain

$$\bar{m} = \frac{985 \times 10^2 \text{ Pa/hPa}}{9.807} = 1.004 \times 10^4 \text{ kg m}^{-2}$$

The mass of the atmosphere is

$$\begin{aligned} M_{atm} &= 4\pi R_E^2 \times \bar{m} \\ &= 4\pi \times (6.37 \times 10^6)^2 \text{ m}^2 \times 1.004 \times 10^4 \text{ kg m}^{-2} \\ &= 5.10 \times 10^{14} \text{ m}^2 \times 1.004 \times 10^4 \text{ kg m}^{-2} \\ &= 5.10 \times 10^{18} \text{ kg}^6 \end{aligned}$$

mass of a constituent is computed by weighting its fractional concentration *by volume* by its molecular weight, i.e.,

$$\frac{m_i}{\sum m_i} = \frac{n_i M_i}{\sum n_i M_i} \quad (1.7)$$

where m_i is the mass, n_i the number of molecules, and M_i the molecular weight of the i th constituent, and the summations are over all constituents.

Diatomeric nitrogen (N_2) and oxygen (O_2) are the dominant constituents of the Earth's atmosphere, and argon (Ar) is present in much higher concentrations than the other noble gases (neon, helium, krypton, and xenon). Water vapor, which accounts for roughly 0.25% of the mass of the atmosphere, is a highly variable constituent, with concentrations ranging from around 10 parts per million by volume (ppmv) in the coldest regions of the Earth's atmosphere up to as much as 5% by volume in hot, humid air masses; a range of more than three orders of magnitude. Because of the large variability of water vapor concentrations in air, it is customary to list the percentages of the various constituents in relation to dry air. Ozone concentrations are also highly variable. Exposure to ozone concentrations >0.1 ppmv is considered hazardous to human health.

For reasons that will be explained in §4.4, gas molecules with certain structures are highly effective at trapping outgoing radiation. The most important of these so-called *greenhouse gases* are water vapor, carbon dioxide, and ozone. Trace constituents CH_4 , N_2O , CO, and chlorofluorocarbons (CFCs) are also significant contributors to the greenhouse effect.

Among the atmosphere's trace gaseous constituents are molecules containing carbon, nitrogen, and sulfur atoms that were formerly incorporated into the cells of living organisms. These gases enter the atmosphere through the burning of plant matter and fossil fuels, emissions from plants, and the decay of plants and animals. The chemical transformations that remove these chemicals from the atmosphere involve oxidation, with the hydroxyl (OH) radical playing an important role. Some of the nitrogen and sulfur compounds are converted into particles that are eventually "scavenged" by raindrops, which contribute to acid deposition at the Earth's surface.

1.3.3 Chemical Composition

The atmosphere is composed of a mixture of gases in the proportions shown in **Table 1.1**, where fractional concentration *by volume* is the same as that based on numbers of molecules, or partial pressures exerted by the gases, as will be explained more fully in Section 3.1. The fractional concentration *by*

Table 1.1 Fractional concentrations by volume of the major gaseous constituents of the Earth's atmosphere up to an altitude of 105 km, with respect to dry air

Constituent ^a	Molecular weight	Fractional concentration by volume
Nitrogen (N_2)	28.013	78.08%
Oxygen (O_2)	32.000	20.95%
Argon (Ar)	39.95	0.93%
Water vapor (H_2O)	18.02	0–5%
Carbon dioxide (CO_2)	44.01	380 ppm
Neon (Ne)	20.18	18 ppm
Helium (He)	4.00	5 ppm
Methane (CH_4)	16.04	1.75 ppm
Krypton (Kr)	83.80	1 ppm
Hydrogen (H_2)	2.02	0.5 ppm
Nitrous oxide (N_2O)	56.03	0.3 ppm
Ozone (O_3)	48.00	0–0.1 ppm

^a So called *greenhouse gases* are indicated by bold-faced type. For more detailed information on minor constituents, see Table 5.1.

⁶ When the vertical and meridional variations in g and the meridional variations in the radius of the earth are accounted for, the mass per unit area and the total mass of the atmosphere are $\sim 0.4\%$ larger than the estimates derived here.

Although aerosols and cloud droplets account for only a minute fraction of the mass of the atmosphere, they mediate the condensation of water vapor in the atmospheric branch of the hydrologic cycle, they participate in and serve as sites for important chemical reactions, and they give rise to electrical charge separation and a variety of atmospheric optical effects.

1.3.4 Vertical structure

To within a few percent, the density of air at sea level is 1.25 kg m^{-3} . Pressure p and density ρ decrease nearly exponentially with height, i.e.,

$$p = p_0 e^{-z/H} \quad (1.8)$$

where H , the *e*-folding depth, is referred to as the *scale height* and p_0 is the pressure at some reference level, which is usually taken as sea level ($z = 0$). In the lowest 100 km of the atmosphere, the scale height ranges roughly from 7 to 8 km. Dividing Eq. (1.8) by p_0 and taking the natural logarithms yields

$$\ln \frac{p}{p_0} \approx -\frac{z}{H} \quad (1.9)$$

This relationship is useful for estimating the height of various pressure levels in the Earth's atmosphere.

Exercise 1.2 At approximately what height above sea level \bar{z}_m does half the mass of the atmosphere lie above and the other half lie below? [Hint: Assume an exponential pressure dependence with $H = 8 \text{ km}$ and neglect the small vertical variation of g with height.]

Solution: Let \bar{p}_m be the pressure level that half the mass of the atmosphere lies above and half lies below. The pressure at the Earth's surface is equal to the weight (per unit area) of the overlying column of air. The same is true of the pressure at any level in the atmosphere. Hence, $\bar{p}_m = \bar{p}_0/2$ where \bar{p}_0 is the global-mean sea-level pressure. From Eq. (1.9)

$$\bar{z}_m = -H \ln 0.5 = H \ln 2$$

Substituting $H = 8 \text{ km}$, we obtain

$$\bar{z}_m = 8 \text{ Km} \times 0.693 \sim 5.5 \text{ km}$$

Because the pressure at a given height in the atmosphere is a measure of the mass that lies above that level, it is sometimes used as a vertical coordinate in lieu of height. In terms of mass, the 500-hPa level, situated at a height of around 5.5 km above sea level, is roughly halfway up to the top of the atmosphere. ■

Density decreases with height in the same manner as pressure. These vertical variations in pressure and density are much larger than the corresponding horizontal and time variations. Hence it is useful to define a *standard atmosphere*, which represents the horizontally and temporally averaged structure of the atmosphere as a function of height only, as shown in Fig. 1.8. The nearly exponential height dependence of pressure and density can be inferred from the fact that the observed vertical profiles of pressure and density on these semilog plots closely resemble straight lines. The reader is invited to verify in Exercise 1.14 at the end of this chapter that the corresponding 10-folding depth for pressure and density is $\sim 17 \text{ km}$.

Exercise 1.3 Assuming an exponential pressure and density dependence with $H = 7.5 \text{ km}$, estimate the heights in the atmosphere at which (a) the air density is equal to 1 kg m^{-3} and (b) the height at which the pressure is equal to 1 hPa.

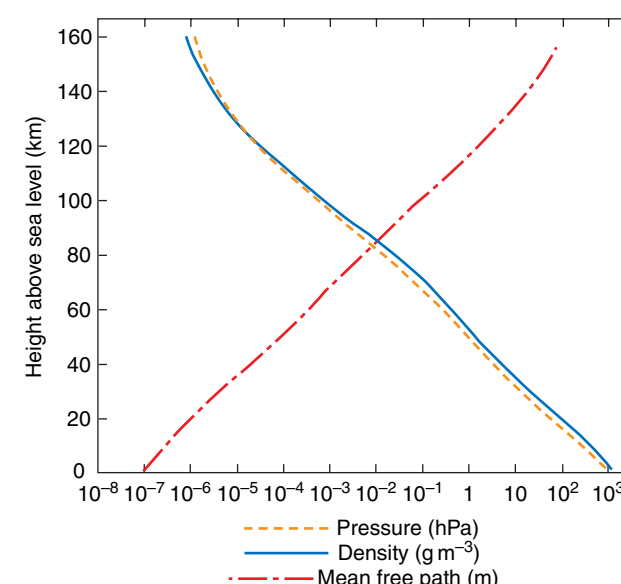


Fig. 1.8 Vertical profiles of pressure in units of hPa, density in units of kg m^{-3} , and mean free path (in meters) for the U.S. Standard Atmosphere.

10 Introduction and Overview

Solution: Solving Eq. (1.9), we obtain $z = H \ln(p_0/p)$, and similarly for density. Hence, the heights are (a)

$$7.5 \text{ km} \times \ln\left(\frac{1.25}{1.00}\right) = 1.7 \text{ km}$$

for the 1-kg m⁻³ density level and (b)

$$7.5 \text{ km} \times \ln\left(\frac{1000}{1.00}\right) = 52 \text{ km}$$

for the 1-hPa pressure level. Because H varies with height, geographical location, and time, and the reference values ρ_0 and p_0 also vary, these estimates are accurate only to within $\sim 10\%$. ■

Exercise 1.4 Assuming an exponential pressure and density dependence, calculate the fraction of the total mass of the atmosphere that resides between 0 and 1 scale height, 1 and 2 scale heights, 2 and 3 scale heights, and so on above the surface.

Solution: Proceeding as in Exercise 1.2, the fraction of the mass of the atmosphere that lies between 0 and 1, 1 and 2, 2 and 3, and so on scale heights above the Earth's surface is $e^{-1}, e^{-2}, \dots e^{-N}$ from which it follows that the fractions of the mass that reside in the 1st, 2nd . . . , N^{th} scale height above the surface are $1 - e^{-1}, e^{-1}(1 - e^{-1}), e^{-2}(1 - e^{-1}) \dots, e^{-N}(1 - e^{-1})$, where N is the height of the base of the layer expressed in scale heights above the surface. The corresponding numerical values are 0.632, 0.233, 0.086 . . . ■

Throughout most of the atmosphere the concentrations of N₂, O₂, Ar, CO₂, and other long-lived constituents tend to be quite uniform and largely independent of height due to mixing by turbulent fluid motions.⁷ Above ~ 105 km, where the mean free path between molecular collisions exceeds 1 m (Fig. 1.8), individual molecules are sufficiently mobile that each molecular species behaves as if it alone were present. Under these conditions, concentrations of heavier constituents decrease more rapidly with height than those of lighter constituents: the density of each constituent drops off exponentially with height, with a scale height inversely proportional to

molecular weight, as explained in Section 3.2.2. The upper layer of the atmosphere in which the lighter molecular species become increasingly abundant (in a relative sense) with increasing height is referred to as the *heterosphere*. The upper limit of the lower, well-mixed regime is referred to as the *turbopause*, where *turbo* refers to turbulent fluid motions and *pause* connotes limit of.

The composition of the outermost reaches of the atmosphere is dominated by the lightest molecular species (H, H₂, and He). During periods when the sun is active, a very small fraction of the hydrogen atoms above 500 km acquire velocities high enough to enable them to escape from the Earth's gravitational field during the long intervals between molecular collisions. Over the lifetime of the Earth the leakage of hydrogen atoms has profoundly influenced the chemical makeup of the Earth system, as discussed in Section 2.4.2.

The vertical distribution of temperature for typical conditions in the Earth's atmosphere, shown in Fig. 1.9, provides a basis for dividing the atmosphere into four layers (*troposphere*, *stratosphere*,

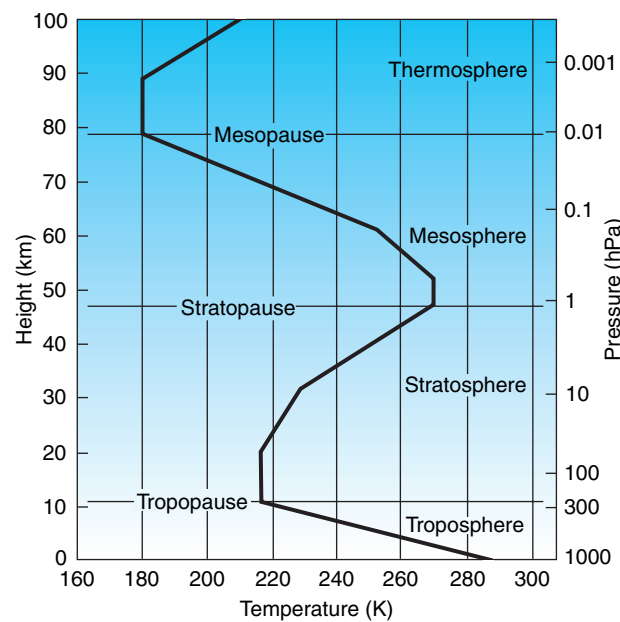


Fig. 1.9 A typical midlatitude vertical temperature profile, as represented by the U.S. Standard Atmosphere.

⁷ In contrast, water vapor tends to be concentrated within the lowest few kilometers of the atmosphere because it condenses and precipitates out when air is lifted. Ozone are other highly reactive trace species exhibit heterogeneous distributions because they do not remain in the atmosphere long enough to become well mixed.

mesosphere, and *thermosphere*), the upper limits of which are denoted by the suffix *pause*.

The *tropo*(turning or changing)*sphere* is marked by generally decreasing temperatures with height, at an average *lapse rate*, of $\sim 6.5 \text{ }^{\circ}\text{C km}^{-1}$. That is to say,

$$\Gamma \equiv \frac{\partial T}{\partial z} \sim 6.5 \text{ }^{\circ}\text{C km}^{-1} = 0.0065 \text{ }^{\circ}\text{C m}^{-1}$$

where T is temperature and Γ is the lapse rate. Tropospheric air, which accounts for $\sim 80\%$ of the mass of the atmosphere, is relatively well mixed and it is continually being cleansed or scavenged of aerosols by cloud droplets and ice particles, some of which subsequently fall to the ground as rain or snow. Embedded within the troposphere are thin layers in which temperature increases with height (i.e., the lapse rate Γ is negative). Within these so-called *temperature inversions* it is observed that vertical mixing is strongly inhibited.

Within the *strato*-(layered)-*sphere*, vertical mixing is strongly inhibited by the increase of temperature with height, just as it is within the much thinner temperature inversions that sometimes form within the troposphere. The characteristic anvil shape created by the spreading of cloud tops generated by intense thunderstorms and volcanic eruptions when they reach the tropopause level, as illustrated in Fig. 1.10, is due to this strong stratification.

Cloud processes in the stratosphere play a much more limited role in removing particles injected by



Fig. 1.10 A distinctive “anvil cloud” formed by the spreading of cloud particles carried aloft in an intense updraft when they encounter the tropopause. [Photograph courtesy of Rose Toomer and Bureau of Meteorology, Australia.]

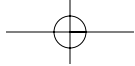
volcanic eruptions and human activities than they do in the troposphere, so residence times of particles tend to be correspondingly longer in the stratosphere. For example, the hydrogen bomb tests of the 1950s and early 1960s were followed by hazardous radioactive fallout events involving long-lived stratospheric debris that occurred as long as 2 years after the tests.

Stratospheric air is extremely dry and ozone rich. The absorption of solar radiation in the ultraviolet region of the spectrum by this *stratospheric ozone layer* is critical to the habitability of the Earth. Heating due to the absorption of ultraviolet radiation by ozone molecules is responsible for the temperature maximum $\sim 50 \text{ km}$ that defines the stratopause.

Above the ozone layer lies the *mesosphere* (meso connoting “in between”), in which temperature decreases with height to a minimum that defines the *mesopause*. The increase of temperature with height within the *thermosphere* is due to the absorption of solar radiation in association with the dissociation of diatomic nitrogen and oxygen molecules and the stripping of electrons from atoms. These processes, referred to as *photodissociation* and *photoionization*, are discussed in more detail in Section 4.4.3. Temperatures in the Earth’s outer thermosphere vary widely in response to variations in the emission of ultraviolet and x-ray radiation from the sun’s outer atmosphere.

At any given level in the atmosphere temperature varies with latitude. Within the troposphere, the *climatological-mean* (i.e., the average over a large number of seasons or years), *zonally averaged* temperature generally decreases with latitude, as shown in Fig. 1.11. The meridional temperature gradient is substantially stronger in the winter hemisphere where the polar cap region is in darkness. The tropopause is clearly evident in Fig. 1.11 as a discontinuity in the lapse rate. There is a break between the tropical tropopause, with a mean altitude $\sim 17 \text{ km}$, and the extratropical tropopause, with a mean altitude $\sim 10 \text{ km}$. The tropical tropopause is remarkably cold, with temperatures as low as $-80 \text{ }^{\circ}\text{C}$. The remarkable dryness of the air within the stratosphere is strong evidence that most of it has entered by way of this “cold trap.”

Exercise 1.5 Based on data shown in Fig. 1.10, estimate the mean lapse rate within the tropical troposphere.



12 Introduction and Overview

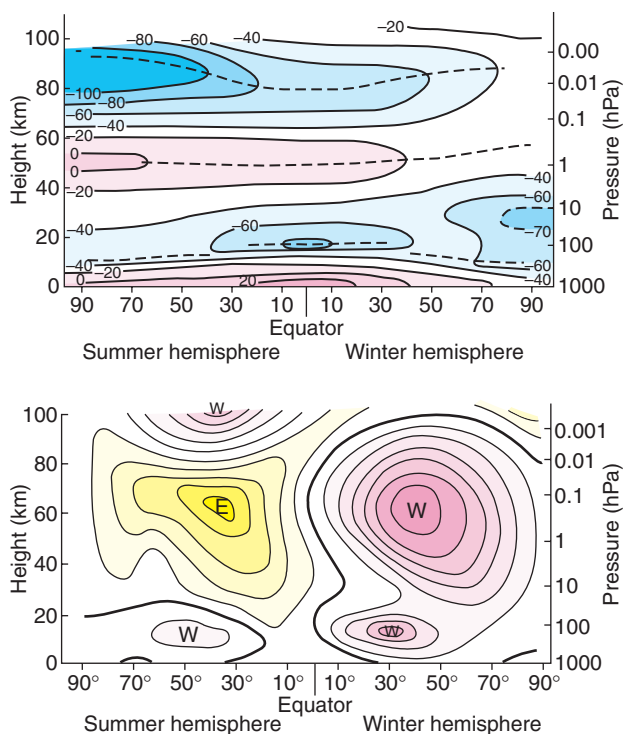


Fig. 1.11 Idealized meridional cross sections of zonally averaged temperature (in °C) (Top) and zonal wind (in m s^{-1}) (Bottom) around the time of the solstices, when the meridional temperature contrasts and winds are strongest. The contour interval is $20\text{ }^{\circ}\text{C}$; pink shading denotes relatively warm regions, and cyan shading relatively cold regions. The contour interval is 10 m s^{-1} ; the zero contour is bold; pink shading and “W” labels denote westerlies, and yellow shading and “E” labels denote easterlies. Dashed lines indicate the positions of the tropopause, stratopause, and mesopause. This representation ignores the more subtle distinctions between northern and southern hemisphere climatologies. [Courtesy of Richard J. Reed.]

Solution: At sea level the mean temperature of the tropics is $\sim 27\text{ }^{\circ}\text{C}$, the tropopause temperature is near $-80\text{ }^{\circ}\text{C}$, and the altitude of the tropopause altitude is $\sim 17\text{ km}$. Hence the lapse-rate is roughly

$$\frac{[27 - (-80)]\text{ }^{\circ}\text{C}}{17\text{ km}} = 6.3\text{ }^{\circ}\text{C km}^{-1}$$

Note that a decrease in temperature with height is implicit in the term (and definition of) *lapse rate*, so the algebraic sign of the answer is positive. ■

1.3.5 Winds

Differential heating between low and high latitudes gives rise to atmospheric motions on a wide range of scales. Prominent features of the so-called *atmospheric general circulation* include planetary-scale west-to-east (westerly) midlatitude *tropospheric jet streams*, centered at the tropopause break around 30° latitude, and lower *mesospheric jet streams*, both of which are evident in Fig. 1.11. The winds in the tropospheric jet stream blow from the west throughout the year; they are strongest during winter and weakest during summer. In contrast, the mesospheric jet streams undergo a seasonal reversal: during winter they blow from the west and during summer they blow from the east.

Superimposed on the tropospheric jet streams are eastward propagating, *baroclinic waves* that feed upon and tend to limit the north–south temperature contrast across middle latitudes. Baroclinic waves are one of a number of types of *weather systems* that develop spontaneously in response to *instabilities* in the large-scale flow pattern in which they are embedded. The low level flow in baroclinic waves is dominated by *extratropical cyclones*, an example of which is shown in Fig. 1.12. The term *cyclone* denotes a closed circulation in which the air spins in the same sense as the Earth’s rotation as viewed from above (i.e., counterclockwise in the northern hemisphere). At low levels the air spirals inward toward the center.⁸ Much of the significant weather associated with extratropical cyclones is concentrated within narrow *frontal zones*, i.e., bands, a few tens of kilometers in width, characterized by strong horizontal temperature contrasts. Extratropical weather systems are discussed in Section 8.1.

Tropical cyclones (Fig. 1.13) observed at lower latitudes derive their energy not from the north–south temperature contrast, but from the release of latent heat of condensation of water vapor in deep convective clouds, as discussed in Section 8.3. Tropical cyclones tend to be tighter and more axisymmetric than extratropical cyclones, and some of them are much more intense. A distinguishing feature of a well-developed tropical cyclone is the relatively calm, cloud-free *eye* at the center.

⁸ The term *cyclone* derives from the Greek word for “coils of a snake.”

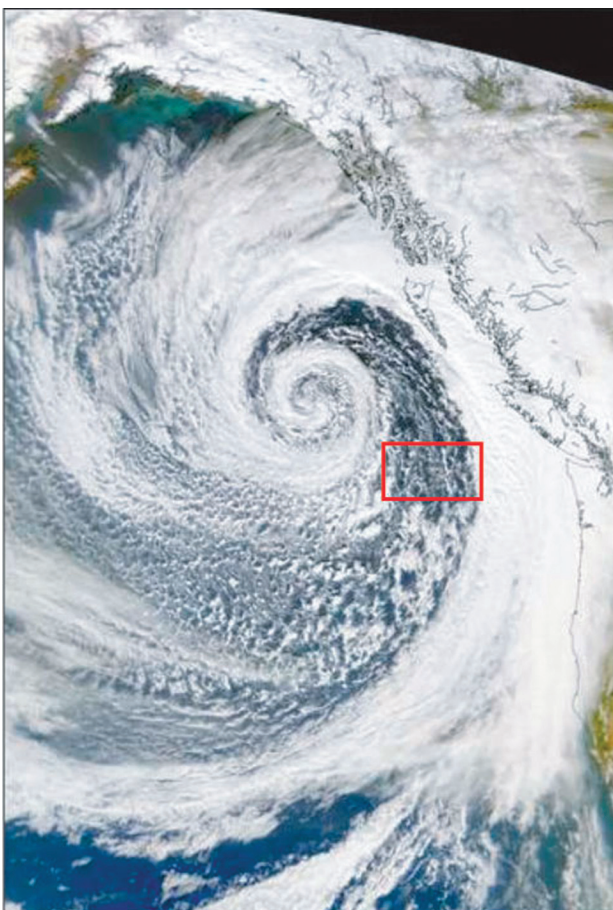


Fig. 1.12 An intense extratropical cyclone over the North Pacific. The spiral cloud pattern, with a radius of nearly 2000 km, is shaped by a vast counterclockwise circulation around a deep low pressure center. Some of the elongated cloud bands are associated with frontal zones. The region enclosed by the red rectangle is shown in greater detail in Fig. 1.21. [NASA MODIS imagery. Photograph courtesy of NASA.]

a. Wind and pressure

The pressure field is represented on weather charts in terms of a set of *isobars* (i.e., lines or contours along which the pressure is equal to a constant value) on a horizontal surface, such as sea level. Isobars are usually plotted at uniform increments: for example, every 4 hPa on a sea-level pressure chart (e.g., ... 996, 1000, 1004 ... hPa). Local maxima in the pressure field are referred to as *high pressure*



Fig. 1.13 The cloud pattern associated with an intense tropical cyclone approaching Florida. The eye is clearly visible at the center of the storm. The radius of the associated cloud system is ~600 km. [NOAA GOES imagery. Photograph courtesy of Harold F. Pierce, NASA Goddard Space Flight Center.]

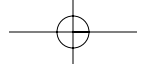
centers or simply *highs*, denoted by the symbol **H**, and minima as *lows* (**L**). At any point on a pressure chart the local *horizontal pressure gradient* is oriented perpendicular to the isobars and is directed from lower toward higher pressure. The strength of the horizontal pressure gradient is inversely proportional to the horizontal spacing between the isobars in the vicinity of that point.

With the notable exception of the equatorial belt (10°S – 10°N), the winds observed in the Earth's atmosphere closely parallel the isobars. In the northern hemisphere, lower pressure lies to the left of the wind (looking downstream) and higher pressure to the right.^{9,10} It follows that air circulates counterclockwise around lows and clockwise around highs, as shown in the right-hand side of Fig. 1.14. In the southern hemisphere the relationships are in the opposite sense, as indicated in the left-hand side of Fig. 1.14.

This seemingly confusing set of rules can be simplified by replacing the words "clockwise" and

⁹ This relationship was first noted by Buys-Ballot in 1857, who stated: If, in the northern hemisphere, you stand with your back to the wind, pressure is lower on your left hand than on your right.

¹⁰ **Christopher H. D. Buys-Ballot** (1817–1890) Dutch meteorologist, professor of mathematics at the University of Utrecht. Director of Dutch Meteorological Institute (1854–1887). Labored unceasingly for the widest possible network of surface weather observations.



14 Introduction and Overview

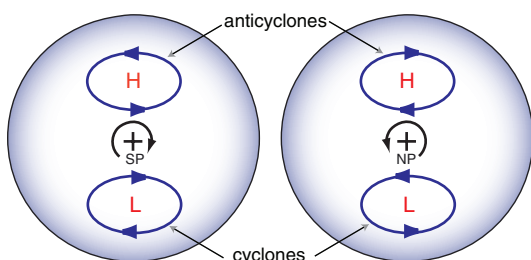


Fig. 1.14 Blue arrows indicate the sense of the circulation around highs (H) and lows (L) in the pressure field, looking down on the South Pole (left) and the North Pole (right). Small arrows encircling the poles indicate the sense of the Earth's rotation.

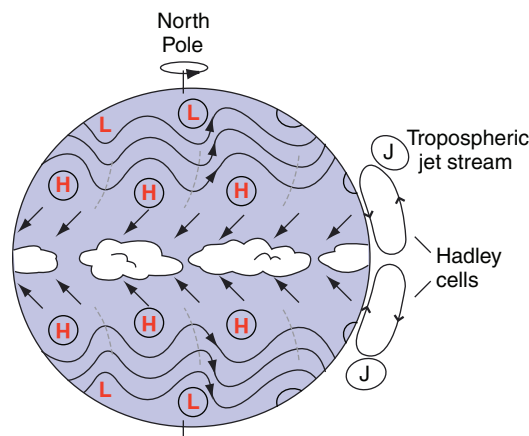


Fig. 1.15 Schematic depiction of sea-level pressure isobars and surface winds on an idealized *aqua planet*, with the sun directly overhead on the equator. The rows of H's denote the subtropical high-pressure belts, and the rows of L's denote the subpolar low-pressure belt. Hadley cells and tropospheric jet streams (J) are also indicated.

“counterclockwise” with the terms *cyclonic* and *anticyclonic* (i.e., in the same or in the opposite sense as the Earth's rotation, looking down on the pole). A *cyclonic circulation* denotes a counterclockwise circulation in the northern hemisphere and a clockwise circulation in the southern hemisphere. In either hemisphere the circulation around low pressure centers is cyclonic, and the circulation around high pressure centers is anticyclonic: that is to say, in reference to the pressure and wind fields, the term *low* is synonymous with *cyclone* and *high* with *anticyclone*.

In the equatorial belt the wind tends to blow straight down the pressure gradient (i.e., directly across the isobars from higher toward lower pressure). In the surface wind field there is some tendency for *cross-isobar flow* toward lower pressure at higher latitudes as well, particularly over land. The basis for these relationships is discussed in Chapter 7.

b. The observed surface wind field

This subsection summarizes the major features of the geographically and seasonally varying *climatological-mean* surface wind field (i.e., the background wind field upon which transient weather systems are superimposed). It is instructive to start by considering the circulation on an idealized ocean-covered Earth with the sun directly overhead at the equator, as inferred from simulations with numerical models.

The main features of this idealized “aqua-planet, perpetual equinox” circulation are depicted in Fig. 1.15. The extratropical circulation is dominated by *westerly wind belts*, centered around 45°N and 45°S . The westerlies are disturbed by an endless succession of eastward migrating disturbances called *baroclinic waves*, which cause the weather at these latitudes to vary from day to day. The average wavelength of these waves is $\sim 4000\text{ km}$ and they propagate eastward at a rate of $\sim 10\text{ m s}^{-1}$.

The tropical circulation in the aqua-planet simulations is dominated by much steadier *trade winds*,¹¹ marked by an easterly zonal wind component and a component directed toward the equator. The *north-easterly trade winds* in the northern hemisphere and the *southeasterly trade winds* in the southern hemisphere are the surface manifestation of overturning circulations that extend through the depth of the troposphere. These so-called *Hadley*¹² cells are characterized by (1) equatorward flow in the boundary layer, (2) rising motion within a few degrees of the equator, (3) poleward return flow in the tropical upper troposphere, and (4) sinking motion in the

¹¹ The term *trade winds* or simply *trades* derives from the steady, dependable northeasterly winds that propelled sailing ships along the popular trade route across the tropical North Atlantic from Europe to the Americas.

¹² **George Hadley** (1685–1768) English meteorologist. Originally a barrister. Formulated a theory for the trade winds in 1735 which went unnoticed until 1793 when it was discovered by John Dalton. Hadley clearly recognized the importance of what was later to be called the Coriolis force.

subtropics, as indicated in Fig. 1.15. Hadley cells and trade winds occupy the same latitude belts.

In accord with the relationships between wind and pressure described in the previous subsection, trade winds and the extratropical westerly wind belt in each hemisphere in Fig. 1.15 are separated by a *subtropical high-pressure belt* centered $\sim 30^\circ$ latitude in which the surface winds tend to be weak and erratic. The jet streams at the tropopause (12 km; 250 hPa) level are situated directly above the subtropical high pressure belts at the Earth's surface. A weak minimum in sea-level pressure prevails along the equator, where trade winds from the northern and southern hemispheres converge. Much deeper lows form in the extratropics and migrate toward the poleward flank of the extratropical westerlies to form the *subpolar low pressure belts*.

In the real world, surface winds tend to be stronger over the oceans than over land because they are not slowed as much by surface friction. Over the Atlantic and Pacific Oceans, the surface winds mirror many of the features in Fig. 1.15, but a longitudinally dependent structure is apparent as well. The subtropical high-pressure belt, rather than being continuous, manifests itself as distinct high-pressure centers, referred to as *subtropical anticyclones*, centered over the mid-oceans, as shown in Fig. 1.16.

In accord with the relationships between wind and pressure described in the previous subsection, surface winds at lower latitudes exhibit an equatorward

component on the eastern sides of the oceans and a poleward component on the western sides. The equatorward surface winds along the eastern sides of the oceans carry (or *advekt*) cool, dry air from higher latitudes into the subtropics; they drive coastal ocean currents that advect cool water equatorward; and they induce coastal upwelling of cool, nutrient-rich ocean water, as explained in the next chapter. On the western sides of the Atlantic and Pacific Oceans, poleward winds advect warm, humid, tropical air into middle latitudes.

In an analogous manner, the subpolar low-pressure belt manifests itself as mid-ocean cyclones referred to, respectively, as the *Icelandic low* and the *Aleutian low*. The poleward flow on the eastern flanks of these semipermanent, subpolar cyclones moderates the winter climates of northern Europe and the Pacific coastal zone poleward of $\sim 40^\circ$ N. The subtropical anticyclones are most pronounced during summer, whereas the subpolar lows are most pronounced during winter.

The idealized tropical circulation depicted in Fig. 1.15, with the northeasterly and southeasterly trade winds converging along the equator, is not realized in the real atmosphere. Over the Atlantic and Pacific Oceans, the trade winds converge, not along the equator, but along $\sim 7^\circ$ N, as depicted schematically in the upper panel of Fig. 1.17. The belt in which the convergence takes place is referred to as the *intertropical convergence zone (ITCZ)*. The asymmetry with respect to the equator is a consequence of the land-sea geometry, specifically the northwest-southeast orientation of the west coastlines of the Americas and Africa.

Surface winds over the tropical Indian Ocean are dominated by the seasonally reversing *monsoon circulation*,¹³ consisting of a broad arc originating as a westward flow in the winter hemisphere, crossing the equator, and curving eastward to form a belt of moisture-laden westerly winds in the summer hemisphere, as depicted [for the northern hemisphere (i.e., boreal) summer] in the lower panel of Fig. 1.17. The monsoon is driven by the presence of India and southeast Asia in the northern hemisphere subtropics versus the southern hemisphere subtropics. Surface temperatures over land respond much more strongly to the seasonal variations in solar heating than those over ocean. Hence, during July the

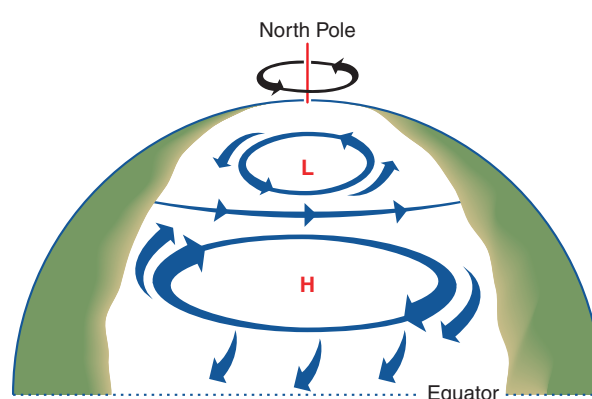
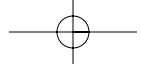


Fig. 1.16 Schematic of the surface winds and sea-level pressure maxima and minima over the Atlantic and Pacific Oceans showing subtropical anticyclones, subpolar lows, the midlatitude westerly belt, and trade winds.

¹³ From *mausin*, the Arabic word for season.



16 Introduction and Overview

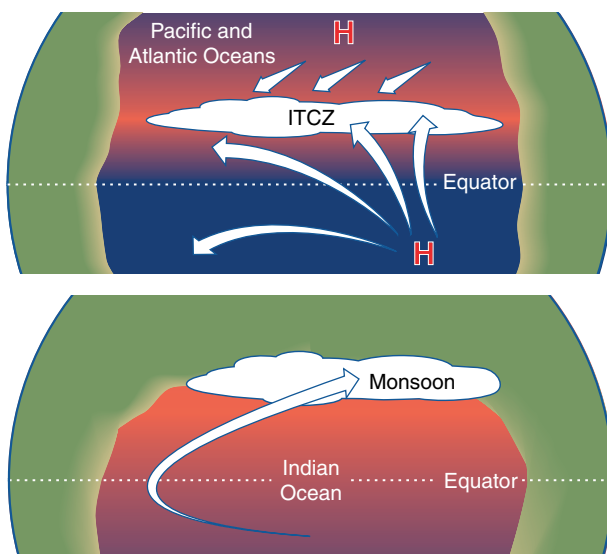


Fig. 1.17 Schematic depicting surface winds (arrows), rainfall (cloud masses), and sea surface temperature over the tropical oceans between $\sim 30^{\circ}\text{N}$ and 30°S . Pink shading denotes warmer, blue cooler sea surface temperature, and khaki shading denotes land. (Top) Atlantic and Pacific sectors where the patterns are dominated by the intertropical convergence zone (ITCZ) and the equatorial dry zone to the south of it. (Bottom) Indian Ocean sector during the northern (boreal) summer monsoon, with the Indian subcontinent to the north and open ocean to the south. During the austral summer (not shown) the flow over the Indian Ocean is in the reverse direction and the rain belt lies just to the south of the equator.

subtropical continents of the northern hemisphere are much warmer than the sea surface temperature over the tropical Indian Ocean. It is this temperature contrast that drives the monsoon flow depicted in the lower panel of Fig. 1.17. In January, when India and southeast Asia are cooler than the sea surface temperature over the tropical Indian Ocean, the monsoon flow is in the reverse sense (not shown).

The reader is invited to compare the observed climatological-mean surface winds for January and July shown in Figs. 1.18 and 1.19 with the idealized flow patterns shown in the two previous figures. In Fig. 1.18, surface winds, based on satellite data, are shown together with the rainfall distribution, indicated by shading, and in Fig. 1.19 a different version of the surface wind field, derived from a blending of many datasets, is superimposed on the climatological-mean sea-level pressure field.

By comparing the surface wind vectors with the shading in Fig. 1.18, it is evident that the major rain belts, which are discussed in the next subsection, tend

to be located in regions where the surface wind vectors flow together (i.e., converge). Convergence at low levels in the atmosphere is indicative of ascending motion aloft. Through the processes discussed in Chapter 3, lifting of air leads to condensation of water vapor and ultimately to precipitation. Figure 1.19 provides verification that the surface winds tend to blow parallel to the isobars, except in the equatorial belt. At all latitudes a systematic drift across the isobars from higher toward lower pressure is also clearly apparent.

The observed winds over the southern hemisphere (Figs. 1.18 and 1.19) exhibit well-defined extratropical westerly and tropical trade wind belts reminiscent of those in the idealized aqua-planet simulations (Fig. 1.15). Over the northern hemisphere the surface winds are strongly influenced by the presence of high latitude continents. The subpolar low-pressure belt manifests itself as oceanic pressure minima (the *Icelandic* and *Aleutian lows*) surrounded by cyclonic (counterclockwise) circulations, as discussed in connection with Fig. 1.16. These features and the belts of westerly winds to the south of them are more pronounced during January than during July. In contrast, the northern hemisphere oceanic subtropical anticyclones are more clearly discernible during July.

c. Motions on smaller scales

Over large areas of the globe, the heating of the Earth's surface by solar radiation gives rise to buoyant plumes analogous to those rising in a pan of water heated from below. As the plumes rise, the displaced air subsides slowly, creating a two-way circulation. Plumes of rising air are referred to by glider pilots as *thermals*, and when sufficient moisture is present they are visible as cumulus clouds (Fig. 1.20). When the overturning circulations are confined to the lowest 1 or 2 km of the atmosphere (the so-called *mixed layer* or *atmospheric boundary layer*), as is often the case, they are referred to as *shallow convection*. Somewhat deeper, more vigorous convection gives rise to showery weather in cold air masses flowing over a warmer surface (Fig. 1.21).

Under certain conditions, buoyant plumes originating near the Earth's surface can break through the weak temperature inversion that usually caps the mixed layer, giving rise to towering clouds that extend all the way to the tropopause, as shown in Fig. 1.22. These clouds are the signature of *deep convection*,

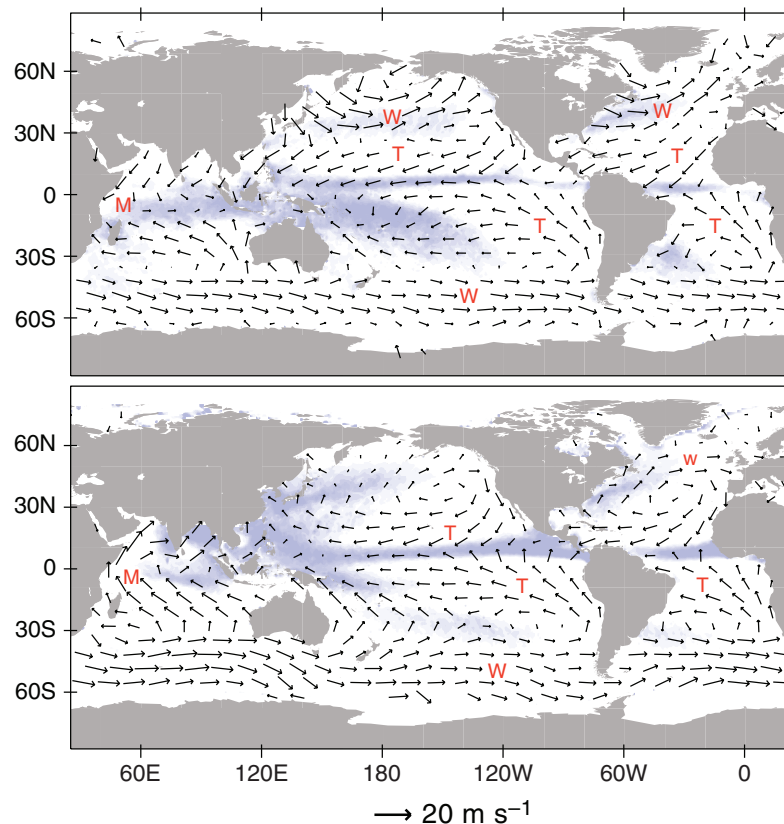
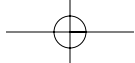


Fig. 1.18 December–January–February and June–July–August surface winds over the oceans based on 3 years of satellite observations of capillary waves on the ocean surface. The bands of lighter shading correspond to the major rain belts. **M**'s denote monsoon circulations, **W**'s westerly wind belts, and **T**'s trade winds. The wind scale is at the bottom of the figure. [Based on QuikSCAT data. Courtesy of Todd P. Mitchell.]

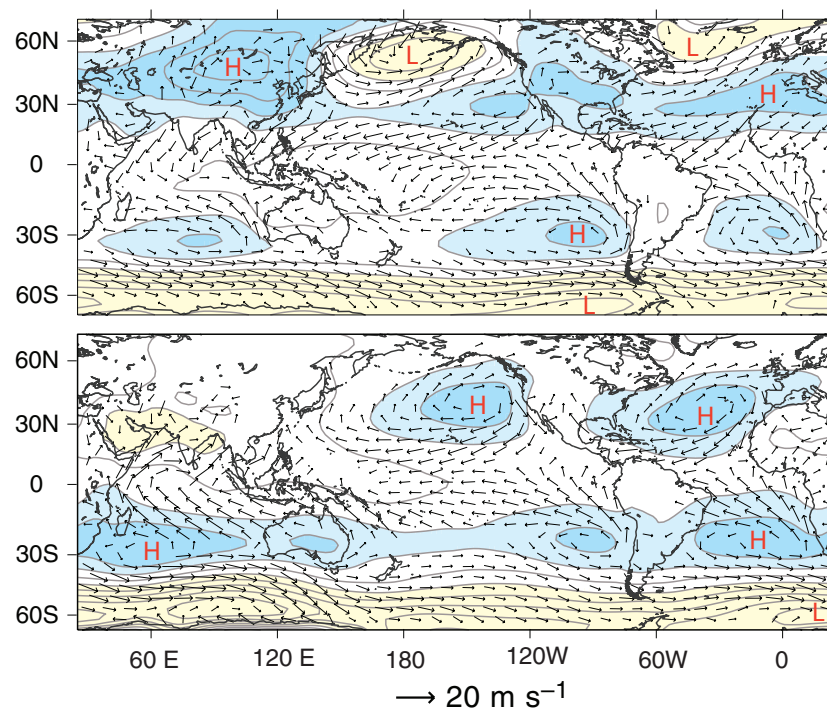
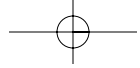


Fig. 1.19 December–January–February (top) and June–July–August (bottom) surface winds, as in Fig. 1.18, but superimposed on the distribution of sea-level pressure. The contour interval for sea-level pressure is 5 hPa. Pressures above 1015 hPa are shaded blue, and pressures below 1000 hPa are shaded yellow. The wind scale is at the bottom of the figure. [Based on the NCEP/NCAR reanalyses. Courtesy of Todd P. Mitchell.]



18 Introduction and Overview



Fig. 1.20 Lumpy cumulus clouds reveal the existence of shallow convection that is largely confined to the atmospheric boundary layer. [Photograph courtesy of Bruce S. Richardson.]



Fig. 1.21 Enlargement of the area enclosed by the red rectangle in Fig. 1.12 showing convection in a cold air mass flowing over warmer water. The centers of the convection cells are cloud free, and the cloudiness is concentrated in narrow bands at the boundaries between cells. The clouds are deep enough to produce rain or snow showers. [NASA MODIS imagery. Photograph courtesy of NASA.]



Fig. 1.22 Clouds over the south China Sea as viewed from a research aircraft flying in the middle troposphere. The foreground is dominated by shallow convective clouds, while deep convection is evident in the background. [Photograph courtesy of Robert A. Houze.]

which occurs intermittently in the tropics and in warm, humid air masses in middle latitudes. Organized deep convection can cause locally heavy rainstorms, often accompanied by lightning and sometimes by hail and strong winds.

Convection is not the only driving mechanism for small-scale atmospheric motions. Large-scale flow over small surface irregularities induces an array of chaotic waves and eddies on scales ranging up to a few kilometers. Such *boundary layer turbulence*, the subject of Chapter 9, is instrumental in causing smoke plumes to widen as they age (Fig. 1.23), in limiting the strength of the winds in the atmosphere, and in mixing momentum, energy, and trace constituents between the atmosphere and the underlying surface.

Turbulence is not exclusively a boundary layer phenomenon: it can also be generated by flow instabilities higher in the atmosphere. The cloud pattern shown in Fig. 1.24 reveals the presence of waves that develop spontaneously in layers with strong *vertical wind shear* (layers in which the wind changes rapidly with height in a vectorial sense). These waves amplify and break, much as ocean waves do when they encounter a beach. *Wave breaking* generates smaller scale waves and eddies, which, in turn, become unstable. Through this succession of instabilities, kinetic energy extracted from the large-scale wind field within the planetary boundary layer and within patches of strong vertical wind shear in the free atmosphere gives rise to a spectrum of small-scale



Fig. 1.23 Exhaust plume from the NASA space shuttle launch on February 7, 2001. The widening of the plume as it ages is due to the presence of small-scale turbulent eddies. The curved shape of the plume is due to the change in horizontal wind speed and direction with height, referred to as *vertical wind shear*. The bright object just above the horizon is the moon and the dark shaft is the shadow of the upper, sunlit part of the smoke plume. [Photograph courtesy of Patrick McCracken, NASA headquarters.]

motions extending down to the molecular scale, inspiring Richardson's¹⁴ celebrated rhyme:

Big whirls have smaller whirls that feed on their velocity, and little whirls have lesser whirls, and so on to viscosity . . . in the molecular sense.

Within localized patches of the atmosphere where wave breaking is particularly intense, eddies on



Fig. 1.24 Billows along the top of this cloud layer reveal the existence of breaking waves in a region of strong vertical wind shear. The right-to-left component of the wind is increasing with height. [Courtesy of Brooks Martner.]

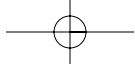
scales of tens of meters can be strong enough to cause discomfort to airline passengers and even, in exceptional cases, to pose hazards to aircraft. Turbulence generated by shear instability is referred to as *clear air turbulence (CAT)* to distinguish it from the turbulence that develops within the cloudy air of deep convective storms.

1.3.6 Precipitation

Precipitation tends to be concentrated in space and time. Annual-mean precipitation at different points on Earth ranges over two orders of magnitude, from a few tens of centimeters per year in dry zones to several meters per year in the belts of heaviest rainfall, such as the ITCZ. Over much of the world climatological-mean precipitation exhibits equally dramatic seasonal variations. The global-mean, annual-mean precipitation rate is ~ 1 m of liquid water per year or ~ 0.275 cm per day or 1 m per year.

Climatological-mean distributions of precipitation for the months of January and July are shown in Fig. 1.25. The narrow bands of heavy rainfall that dominate the tropical Atlantic and Pacific sectors coincide with the ITCZ in the surface wind field. In the Pacific and Atlantic sectors the ITCZ is flanked by expansive *dry zones* that extend westward from the continental deserts and cover much of the subtropical oceans. These features coincide with the

¹⁴ **Lewis F. Richardson** (1881–1953). English physicist and meteorologist. Youngest of seven children of a Quaker tanner. Served as an ambulance driver in France during World War I. Developed a set of finite differences for solving differential equations for weather prediction, but his formulation was not quite correct and at that time (1922) computations of this kind could not be performed quickly enough to be of practical use. Pioneer in the causes of war, which he described in his books “Arms and Insecurity” and “Statistics of Deadly Quarrels,” Boxward Press, Pittsburgh, 1960. Sir Ralph Richardson, the actor, was his nephew.



20 Introduction and Overview

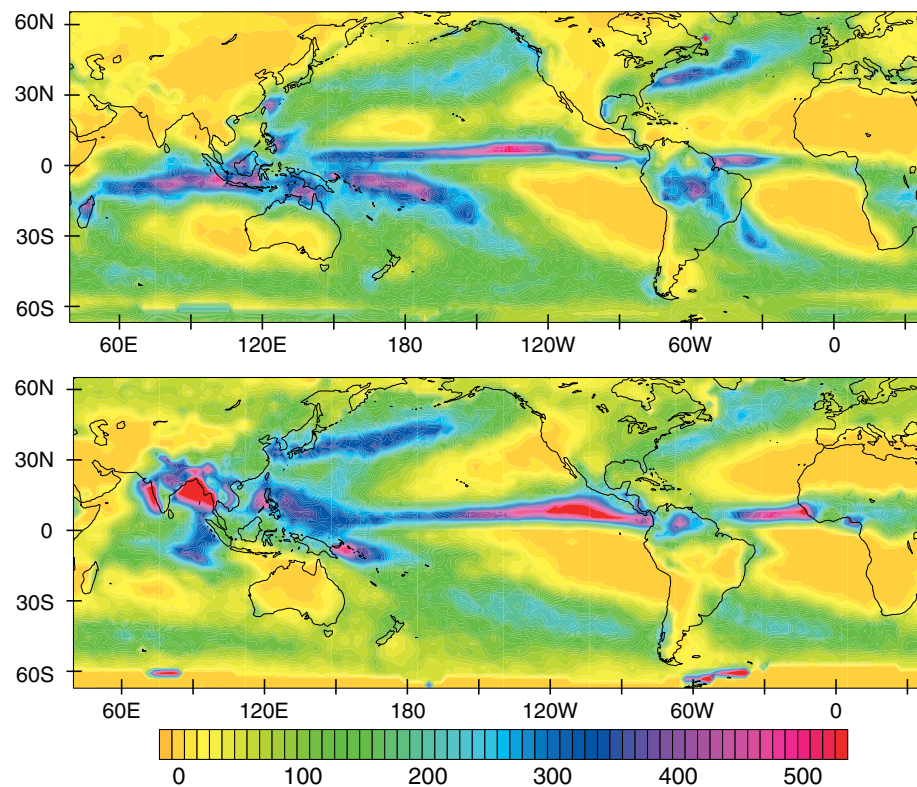


Fig. 1.25 January and July climatological-mean precipitation. [Based on infrared and microwave satellite imagery over the oceans and rain gauge data over land, as analyzed by the NOAA National Centers for Environmental Prediction CMAP project. Courtesy of Todd P. Mitchell.]

subtropical anticyclones and, in the Pacific and Atlantic sectors, they encompass equatorial regions as well.

Small seasonal or year-to-year shifts in the position of the ITCZ can cause dramatic local variations in rainfall. For example, at Canton Island (3°S , 170°W) near the western edge of the equatorial dry zone, rainfall rates vary from zero in some years to over 30 cm per month (month after month) in other years in response to subtle year-to-year variations in sea surface temperature over the equatorial Pacific that occur in association with El Niño, as discussed in Section 10.2.2.

Over the tropical continents, rainfall is dominated by the monsoons, which migrate northward and southward with the seasons, following the sun. Most equatorial regions receive rainfall year-round, but the belts that lie $10 - 20^{\circ}$ away from the equator experience pronounced dry seasons that correspond to the time of year when the sun is overhead in the opposing hemisphere. The rainy season over India and southeast Asia coincides with the time of year in which the surface winds over the northern Indian Ocean blow from the west (Figs. 1.17 and 1.18). Analogous relationships exist

between wind and rainfall in Africa and the Americas. The onset of the rainy season, a cause for celebration in many agricultural regions of the subtropics, is remarkably regular from one year to the next and it is often quite dramatic: for example, in Mumbai (formerly Bombay) on the west coast of India, monthly mean rainfall jumps from less than 2 cm in May to ~ 50 cm in June.

The flow of warm humid air around the western flanks of the subtropical anticyclones brings copious summer rainfall to eastern China and Japan and the eastern United States. In contrast, Europe and western North America and temperate regions of the southern hemisphere experience dry summers. These regions derive most of their annual precipitation from wintertime extratropical cyclones that form within the belts of westerly surface winds over the oceans and propagate eastward over land. The rainfall maxima extending across the Pacific and Atlantic at latitudes $\sim 45^{\circ}\text{N}$ in Fig. 1.25 are manifestations of these oceanic *storm tracks*.

Rainfall data shown in Fig. 1.25, which are averaged over 2.5° latitude $\times 2.5^{\circ}$ longitude grid boxes, do not fully resolve the fine structure of the distribution

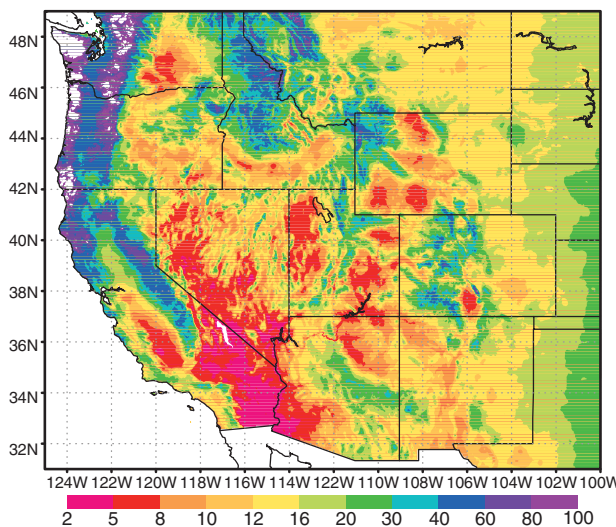


Fig. 1.26 Annual-mean precipitation over the western United States resolved on a 10-km scale making use of a model. The color bar is in units of inches of liquid water (1 in. = 2.54 cm). Much of the water supply is derived from a winter snow pack, which tends to be concentrated in regions of blue, purple, and white shading. [Map produced by the NOAA Western Regional Climate Center using PRISM data from Oregon State University. Courtesy of Kelly Redmond.]

of precipitation in the presence of *orography* (i.e., terrain). Flow over and around mountain ranges imparts a fractal-like structure to the precipitation distribution, with enhanced precipitation in regions where air tends to be lifted over terrain features and suppressed precipitation in and downstream of regions of descent (i.e., *subsidence*).

The distribution of annual-mean precipitation over the western United States, shown in Fig. 1.26,

illustrates the profound influence of orography. Poleward of $\sim 35^\circ$, which corresponds to the equatorward limit of the extratropical westerly flow regime that prevails during the wintertime, annual-mean precipitation tends to be enhanced where moisture-laden marine air is lifted as it moves onshore and across successive ranges of mountains. The regions of suppressed precipitation on the lee side of these ranges are referred to as *rain shadows*.

On any given day, the cloud patterns revealed by global satellite imagery exhibit patches of deep convective clouds that can be identified with the ITCZ and the monsoons over the tropical continents of the summer hemisphere; a relative absence of clouds in the subtropical dry zones; and a succession of comma-shaped, frontal cloud bands embedded in the baroclinic waves tracking across the mid-latitude oceans. These features are all present in the example shown in Fig. 1.27.

1.4 What's Next?

The brief survey of the atmosphere presented in this chapter is just a beginning. All the major themes introduced in this survey are developed further in subsequent chapters. The first section of the next chapter provides more condensed surveys of the other components of the Earth system that play a role in climate: the oceans, the cryosphere, the terrestrial biosphere, and the Earth's crust and mantle.

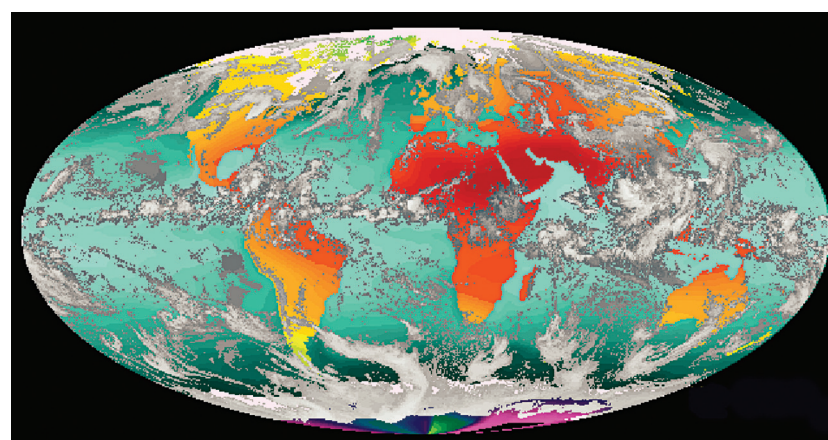
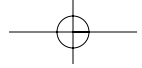


Fig. 1.27 Composite satellite image showing sea surface temperature and land surface air temperature and clouds. [Courtesy of the University of Wisconsin Space Science and Engineering Center.]



22 Introduction and Overview

Exercises¹⁵

1.6 Explain or interpret the following:

- (a) Globally averaged surface pressure is 28 hPa lower than globally averaged sea-level pressure (1013 hPa).
- (b) Density decreases exponentially with height in the atmosphere, whereas it is nearly uniform in the oceans.
- (c) Pressure in the atmosphere and ocean decreases monotonically with height. The height dependence is almost exponential in the atmosphere and linear in the ocean.
- (d) Concentrations of some atmospheric gases, such as N₂, O₂, and CO₂, are nearly uniform below the turbopause, whereas concentrations of other gases such as water vapor and ozone vary by orders of magnitude.
- (e) Below ~ 100 km, radar images of meteor trails become distorted and break up into puffs much like jet aircraft contrails do. In contrast, meteor trails higher in the atmosphere tend to vanish before they have time to become appreciably distorted.
- (f) Airline passengers flying at high latitudes are exposed to higher ozone concentrations than those flying in the tropics.
- (g) In the tropics, deep convective clouds contain ice crystals, whereas shallow convective clouds do not.
- (h) Airliners traveling between Tokyo and Los Angeles often follow a great circle route westbound and a latitude circle eastbound.
- (i) Aircraft landings on summer afternoons tend to be bumpier than nighttime landings, especially on clear days.
- (j) Cumulus clouds like the ones shown in Fig. 1.20 are often observed during the daytime over land when the sky is otherwise clear.

(k) New York experiences warmer, wetter summers than Lisbon, Portugal, which is located at nearly the same latitude.

- 1.7 To what feature in Fig. 1.15 does the colloquial term horse latitudes refer? What is the origin of this term?
- 1.8 Prove that exactly half the area of the Earth lies equatorward of 30° latitude.

- 1.9 How many days would it take a hot air balloon traveling eastward along 40 °N at a mean speed of 15 m s⁻¹ to circumnavigate the globe?

Answer: 23.7 days

- 1.10 Prove that pressure expressed in cgs units of millibars (1 mb = 10⁻³ bar) is numerically equal to pressure expressed in SI units of hPa (1 hPa = 10² Pa).

- 1.11 How far below the surface of the water does a diver experience a pressure of 2 atmospheres (i.e., a doubling of the ambient atmospheric pressure) due to the weight of the overlying water?

Answer: ~ 10 m.

- 1.12 In a sounding taken on a typical winter day at the South Pole the temperature at the ground is -80 °C and the temperature at the top of a 30-m high tower is -50 °C. Estimate the lapse rate within the lowest 30 m, expressed in °C km⁻¹.

Answer: $-1,000$ °C km⁻¹.

- 1.13 “Cabin altitude” in typical commercial airliners is around 1.7 km. Estimate the typical pressure and density of the air in the passenger cabin.¹⁶

Answer: 800 hPa and 1.00 kg m⁻³.

- 1.14 Prove that density and pressure, which decrease more or less exponentially with height, decrease by a factor of 10 over a depth of 2.3 H, where H is the scale height.

- 1.15 Consider a perfectly elastic ball of mass m bouncing up and down on a horizontal surface under the action of a downward gravitational acceleration g. Prove that in the time average over an integral number of bounces, the

¹⁵ A list of constants and conversions that may be useful in working the exercises is printed at the end of the book. Answers and solutions to most of the exercises are provided on the Web site for the book.

¹⁶ Over many generations humans are capable of adapting to living at altitudes as high as 5 km (~ 550 hPa) and surviving for short intervals at altitudes approaching 9 km (~ 300 hPa). The first humans to visit such high latitudes may have been British meteorologist James Glaisher and balloonist Henry Coxwell in 1862. Glaisher lost consciousness for several minutes and Coxwell was barely able to arrest the ascent of the balloon after temporarily losing control.

downward force exerted by the ball upon the surface is equal to the weight of the ball. [Hint: The downward force is equal to the downward momentum imparted to the surface with each bounce divided by the time interval between successive bounces.] Does this result suggest anything about the “weight” of an atmosphere comprised of gas molecules?

- 1.16 Estimate the percentage of the mass of the atmosphere that resides in the stratosphere based on the following information. The mean pressure level of tropical tropopause is around 100 hPa and that of the extratropical tropopause is near 300 hPa. The break between the tropical and the extratropical tropopause occurs near 30° latitude so that exactly half the area of the Earth lies in the tropics and half in the extratropics. On the basis of an inspection of Fig. 1.11, verify that the representation of tropopause height in this exercise is reasonably close to observed conditions.

Answer: 20%.

- 1.17 If the Earth’s atmosphere were replaced by an incompressible fluid whose density was everywhere equal to the atmospheric density observed at sea level (1.25 kg m^{-3}), how deep would it have to be to account for the observed mean surface pressure of $\sim 10^5 \text{ Pa}$?

Answer: 8 km.

- 1.18 The mass of water vapor in the atmosphere ($\sim 100 \text{ kg m}^{-2}$) is equivalent to a layer of liquid water how deep?

Answer: $\sim 1 \text{ cm}$.

- 1.19 Assuming that the density of air decreases exponentially with height from a value of 1.25 kg m^{-3} at sea level, calculate the scale height that is consistent with the observed global mean surface pressure of $\sim 10^3 \text{ hPa}$. [Hint: Write an expression analogous to (1.8) for density and integrate it from the Earth’s surface to infinity to obtain the atmospheric mass per unit area.]

Answer: 8 km.

- 1.20 The equatorward flow in the trade winds averaged around the circumference of the Earth at 15°N and 15°S is $\sim 1 \text{ m s}^{-1}$. Assume that this flow extends through a layer extending from sea

level up to the 850-hPa pressure surface. Estimate the equatorward mass flux into the equatorial zone. [Hint: The equatorward mass flux across the 15°N , in units of kg s^{-1} , is given by

$$-\oint_{15^\circ\text{N}} \int_0^{z=850} \rho v dz dx$$

where ρ is the density of the air, v is the meridional (northward) velocity component, the line integral denotes an integration around the 15°N latitude circle, and the vertical integral is from sea level up to the height of the 850-hPa surface. Evaluate the integral, making use of the relations

$$\oint_{15^\circ\text{N}} dx = 2\pi R_E \cos 15^\circ$$

and

$$\int_0^{z=850} \rho dz = \frac{(1000 - 850) \text{ hPa} \times 100 \text{ Pa/hPa}}{g}.$$

Answer: $1.18 \times 10^{11} \text{ kg s}^{-1}$.

- 1.21 During September, October, and November the mean surface pressure over the northern hemisphere increases at a rate of $\sim 1 \text{ hPa}$ per month. Calculate the mass averaged northward velocity across the equator

$$v_m \equiv \frac{\oint_0^{\infty} \rho v dz dx}{\oint_0^{\infty} \rho dz dx}$$

that is required to account for this pressure rise.

[Hint: Assume that atmospheric mass is conserved, i.e., that the pressure rise in the northern hemisphere is entirely due to the influx of air from the southern hemisphere.]

Answer: 2.46 mm s^{-1} .

- 1.22 Based on the climatological-mean monthly temperature and rainfall data provided on the compact disk, select several stations that fit into the following climate regimes: (a) equatorial belt, wet year-round; (b) monsoon; (c) equatorial dry zone; (d) extratropical, with dry summers; and (e) extratropical, with wet summers. Locate each station with reference to the features in Figs. 1.18, 1.19, and 1.25.

